

Observational constraints on the progenitor metallicities of core-collapse supernovae[★]

J. P. Anderson,^{1†} R. A. Covarrubias,² P. A. James,³ M. Hamuy¹
and S. M. Habergham³

¹*Departamento de Astronomía, Universidad de Chile, Casilla 36-D, Santiago, Chile*

²*Anglo-Australian Observatory, PO Box 296, Epping, NSW 1710, Australia*

³*Astrophysics Research Institute, Liverpool John Moores University, Twelve Quays House, Egerton Wharf, Birkenhead CH41 1LD*

Accepted 2010 May 28. Received 2010 May 7; in original form 2010 April 2

ABSTRACT

We present constraints on the progenitor metallicities of core-collapse supernovae. To date, nearly all metallicity constraints have been inferred from indirect methods such as metallicity gradients in host galaxies, luminosities of host galaxies or derived global galaxy metallicities. Here, progenitor metallicities are derived from optical spectra taken at the sites of nearby supernovae, from the ratio of strong emission lines found in their host H II regions. We present results from the spectra of 74 host H II regions and discuss the implications that these have on the nature of core-collapse supernova progenitors.

Overall, while we find that the mean metallicity of Type Ibc environments is higher than that of Type II events, this difference is smaller than observed in previous studies. There is only a 0.06 dex difference in the mean metallicity values, at a statistical significance of $\sim 1.5\sigma$, while using a Kolmogorov–Smirnov test we find that the two metallicity distributions are marginally consistent with being drawn from the same parent population (probability > 10 per cent). This argues that progenitor metallicity is not a dominant parameter in deciding supernovae type, with progenitor mass and/or binarity playing a much more significant role.

The mean derived oxygen metallicities [$12 + \log(O/H)$] for the different supernova types, on the Pettini & Pagel scale, are 8.580 (standard error on the mean of 0.027) for the 46 Type II supernovae (dominated by Type II plateau), 8.616 (0.040) for 10 Type Ib and 8.626 (0.039) for 14 Type Ic. Overall, the Type Ibc supernovae have a mean metallicity of 8.635 (0.026, 27 supernovae). Hence, we find a slight suggestion of a metallicity sequence, in terms of increasing progenitor metallicity going from Type II through Ib and finally Ic supernovae arising from the highest metallicity progenitors.

Finally we discuss these results in the context of all current literature progenitor metallicity measurements, and discuss biases and selection effects that may affect the current sample compared to overall supernova and galaxy samples.

Key words: supernovae: general – galaxies: abundances.

1 INTRODUCTION

Whilst supernovae (SNe) continue to be exploited to investigate the nature of the Universe, exact understanding of their progenitor systems and explosion mechanisms, and how these relate to the transient phenomena we observe remain elusive.

Core-collapse (CC) SNe are thought to arise from massive stars ($> 8\text{--}10 M_{\odot}$) that collapse once they have spent their nuclear fuel, the rebounding shock wave of this collapse powering their observed heterogenous light curve and spectral properties. A key goal in current SN research is to provide links between progenitor systems and observed transients.

[★]Based on observations made with the William Herschel Telescope (WHT) operated on the island of La Palma by the Isaac Newton Group in the Spanish Observatorio del Roque de los Muchachos of the Institute de Astrofísica de Canarias; observations obtained with the Apache Point Observatory (APO) 3.5-m telescope, which is owned and operated by the Astrophysical Research Consortium; observations obtained with the Magellan Consortium's Clay Telescope; and observations obtained with the European Southern Observatory (ESO) New Technology Telescope (NTT), proposal ID: 077.C-0414.

†E-mail: anderson@das.uchile.cl

In a series of papers we have attempted to constrain the nature of progenitors through analysis of the stellar populations found in the immediate vicinity of nearby SNe. Here we present constraints on progenitor metallicities derived from emission line spectra of 74 host H II regions.

1.1 Core-collapse supernova progenitors

CC SNe are classified on the basis of properties of their light curves (e.g. Barbon, Ciatti & Rosino 1979), and features found (or lacking) in their optical spectra (see Filippenko 1997 for a review of spectral classifications). The most common CC class are the SNe Type II (SNII). These show hydrogen in their spectra, which is thought to indicate that large portions of their outer envelopes have been retained prior to explosion. SNII are further divided into a number of subtypes. SNIIP are the most abundant CC type and display a long plateau (~ 100 d) in their light curves, while other subtypes (IIL, I Ib, II n) display differences in their light curves and spectra, that indicate differences in the progenitor system and surrounding circumstellar material at the epoch of explosion. The other main CC types are the SNIbc (we use this notation throughout the paper to denote the set of events classified as Ib, Ic or Ib/c in the literature). These types lack any detectable hydrogen emission (hence the classification as I rather than II), while SNIc also lack the helium lines seen in the spectra of SNIb. The absence of these elements is thought to imply a large amount of mass loss by the progenitors of these SNe where they have lost much of their outer envelopes, either due to strong stellar winds or mass transfer in binary systems.

The most direct method for determining the properties of SN progenitors is through their identification on pre-SN images. This has had some success, especially for the abundant SNIIP. Smartt et al. (2009) published a compilation of all progenitor mass estimates for SNIIP available at the time of writing. Using a maximum likelihood analysis of all mass estimates, plus derived upper limits, these authors derive a mass range for SNIIP progenitors of 8.5 to 16.5 M_{\odot} and conclude that SNIIP arise from red supergiant progenitors. While the statistics for the abundant SNIIP are becoming significant (when upper limits are included), only a small number of detections or derived upper limits are available for the other CC subtypes. Those other supernova types of most interest (with respect to the current study) are the SNIbc. If arising from single stars, the proposed progenitors for these SN types are massive Wolf-Rayet (WR) stars (e.g. Gaskell et al. 1986), as these stars have been stripped of most of their outer envelopes, hence lacking hydrogen in their pre-supernova states as required by the spectra of SNIbc. It is also interesting to note the recent study by Leloudas et al. (2010) comparing the spatial distributions of SNe and WR stars within galaxies, with respect to host galaxy g' -band light. These authors find that the distributions of SNIbc explosion sites and WR stars are consistent with being drawn from the same parent population. However, as summarized by Smartt (2009), a direct detection of a progenitor star remains elusive, despite 10 cases of nearby SNIbc with the required pre-SN imaging. An alternative progenitor path for producing SNIbc (i.e. progenitors with stripped envelopes), is through lower mass binaries, where the required mass loss occurs through mass transfer to the secondary star (e.g. Podsiadlowski, Joss & Hsu 1992). This second progenitor path also finds support from the relative frequency SNIbc to SNII, which, when compared to the initial masses of WR stars in the Local Group (Crowther 2007), is incompatible with all SNIbc being produced from single WR progenitor stars. While further direct detections are shedding new light on progenitor characteristics, the requirement of very nearby SNe

means we will have to wait for definitive answers from these studies, especially where the less numerous SNIbc and II subtypes are concerned. Therefore, to complement these studies we must look to other avenues of research to investigate progenitor properties. This is even more pertinent when investigating progenitor metallicities, as currently the direct detection gives little direct evidence for constraining this property.

Host galaxy properties are commonly employed to differentiate between different progenitor scenarios. Indeed, the first separation of SNe into CC and thermonuclear explosions (i.e. coming from young and old stellar populations) arose from the lack of CC SNe and presence of thermonuclear SNIa in early-type elliptical galaxies. More recently, host galaxy properties have been used to infer metallicity differences between SNII and SNIbc (e.g. Prieto, Stanek & Beacom 2008, see the subsequent section for additional discussion), and have been used to derive delay time distributions for SNIa. Our methods used here and in previous papers are intermediate to the above two extremes as we use the properties of the stellar population within galaxies, local to the SN positions, to constrain their progenitor properties.

1.2 Constraints on progenitor metallicities

The first observational evidence for metallicity differences between SNII and SNIbc was presented by van den Bergh (1997) (following initial work by Bartunov, Makarova & Tsvetkov 1992), who showed that SNIbc appeared to be more centrally concentrated than SNII within host galaxies. Metallicity gradients are found in nearly all galaxy types (see Henry & Worthey 1999 for a review), in the sense that higher metallicities are found in galaxy centres. These authors therefore interpreted the increased centralization of SNIbc as indication that they arose from higher metallicity progenitors. Interpretations of higher metallicity progenitors for SNIbc can be understood from a theoretical viewpoint, where higher metallicity stars have higher line-driven winds (e.g. Puls et al. 1996; Kudritzki & Puls 2000; Mokiem et al. 2007), thus the progenitors lose more mass through these winds prior to supernova, hence removing their outer hydrogen and helium envelopes. The radial trends above have been confirmed with increased statistics (see Tsvetkov, Pavlyuk & Bartunov 2004 and most recently Hakobyan et al. 2009), furthering the claim of higher metallicity progenitors for SNIbc. Anderson & James (2009) (hereafter AJ09) investigated the radial distribution of CC SNe with respect to the host galaxy stellar populations (previous studies focused on distances). Similar trends were found with a central concentration of SNIbc with respect to both young and old stellar populations compared with SNII. As above this was ascribed to differences in progenitor metallicities. However, further analysis of this sample (Haberman, Anderson & James 2010, hereafter HAJ10) has complicated these interpretations. Subdividing the host galaxies from AJ09 according to the presence or absence of signs of interaction or disturbance it was found that both SNII and SNIbc are more centrally concentrated in the disturbed/interacting hosts. However, this effect was much more prevalent for the SNIbc than SNII. This was interpreted as evidence for the centralization of star formation (SF) during galaxy interactions, and also the requirement of a top heavy initial mass function (IMF) to explain the relative abundance of SNIbc over SNII. Hence, if these interpretations are corroborated they decrease the probable importance of metallicity effects on the distribution of the different CC SN types.

Other galaxy properties also correlate with metallicity and have been used to further investigate the nature of progenitors. The well-known galaxy luminosity–metallicity relationship was used

by Prantzos & Boissier (2003) and updated in Boissier & Prantzos (2009) to investigate differences in progenitor metallicity between SN types, both on a global host galaxy scale, and a local one using galaxy metallicity gradients. They found a significant difference between the overall SNIi and SNIbc populations, with apparently contradictory results regarding any differences between SNIb and Ic; in global terms Ib were found to arise from more metal rich galaxies, while in terms of local estimations the opposite was true, however these differences were put down to low number statistics.

All the above studies used somewhat indirect methods for inferring progenitor metallicities. A more direct approach is to derive gas-phase metallicities from host galaxy spectra. Prieto et al. (2008) presented host galaxy metallicities for 111 SNe host galaxies (all SN types), derived from Sloan Digital Sky Survey (SDSS) spectra. Again, they found that SNIbc appeared to arise from more metal rich environments than SNIi. However, these metallicities were global rather than local, and therefore do not take into account metallicity gradients found within galaxies, and how these relate to the differing radial positions of different SN types.

For further constraints to be made, we therefore need to derive metallicities *at* the positions SNe are detected. This is the analysis we present here which follows on from a study by Modjaz et al. (2008) who derived metallicities for the immediate environments of broad-line SNIc that were accompanied with long-duration gamma-ray bursts (LGRBs), and those that were not, finding that the former favoured lower metallicity environments. Here we extend this analysis to include all the main CC SN types, with the main aim of comparing the metallicity of SNIi and SNIbc progenitors.

The paper is arranged as follows. In the next section we summarize the data used for this investigation, listing the samples involved and observations obtained. In Section 3, we discuss our host H II region metallicity determinations. In Section 4, we present the results for the different supernova types. In Section 5, we discuss the implications of these results and compare them to those in the current literature. Finally in Section 6 we summarize our main conclusions.

2 DATA

Long-slit spectra were obtained for the host H II regions of 73 CC SNe (plus 1 SN ‘impostor’). The discussion of these data sets below is separated into those obtained with the Intermediate dispersion Spectrograph and Imaging System (ISIS) on the WHT on La Palma, in the Canary Islands, and those obtained at various observatories, which are taken from the thesis work of Ricardo Covarrubias (2007), the results of which (comparing SN luminosities with environment metallicities) will be published elsewhere (Covarrubias et al., in preparation). Many SNIi are found far from bright H II regions (see Anderson & James 2008, hereafter AJ08), and therefore to estimate progenitor metallicities one has to extract spectra away from the catalogued SN positions. Possible biases that are introduced by this procedure are discussed in Section 5.1.

We note here the heterogenous nature of these data sets. The ISIS data are a random selection taken from the SN host galaxy H α imaging sample presented in AJ09. This initial sample, in turn, was a random selection of nearby SNe host galaxies ($<6000 \text{ km s}^{-1}$) taken from the Asiago SN catalogue (Barbon et al. 2009), imaged in H α to investigate the association of the different SN types to a young stellar population. We therefore assume that both that sample and the subset used here are a random selection of *observed* SNe in the nearby Universe. The Covarrubias sample consists of SNIIP that had been extensively followed photometrically to allow characteri-

zation of their light curve properties and for the use of these objects for distance measurements. These objects are, therefore, as above a random selection of SNe discovered through different galaxy targeted searches, and therefore as above are a random sample of (to date) *observed* SNe in the local Universe. There are some cases in this second sample that are taken from galaxies further afield than the ISIS sample, but we do not believe that these small differences will affect the results presented below.

In a perfect world, one would hope to perform such analyses as presented here on a homogeneous SN sample, discovered through an unbiased search campaign. However, due to the proximity of galaxies needed for this type of study (in order to detect individual H II regions, to probe true *local* metallicities), and the to date galaxy targeted nature of nearby searches, this is not currently possible. Hence, we proceed with the current sample and discuss possible biases that may exist in the analysis in Section 5.2.

2.1 ISIS spectra

Long-slit spectra were obtained for 50 CC SN (and 1 SN ‘impostor’) host H II regions over two observing runs with ISIS on the WHT in 2008 February and 2009 February. The details of these observations and the SN host galaxy properties are listed in Table 1. These data were taken with the dichroic in the default position, splitting the incoming light into the red and blue arms at 5300 Å. The R300B grating was employed in the blue giving a spectral dispersion of $0.86 \text{ Å pixel}^{-1}$, and the R316R in the red arm giving a dispersion of $0.93 \text{ Å pixel}^{-1}$. Generally data were taken with a slit width of 1 arcsec, therefore attaining spectral resolutions of $\sim 4 \text{ Å}$ in each arm. However at times we observed in bad conditions and therefore increased the slit width to 2.5 arcsec to increase the target photons reaching the detector, decreasing the spectral resolution but we were still able to resolve H α from the [N II] lines.

Most of these data were not taken at the parallactic angle, either to enable the host H II regions of multiple SNe to be observed or to enable further study into the metallicity gradients within galaxies. While some of the spectra will therefore suffer from atmospheric differential refraction (Filippenko 1982), for metallicity determinations we chose the line ratio diagnostics from Pettini & Pagel (2004, hereafter PP04), who employ line ratios of emission lines close in wavelength and hence negate this issue. Standard reduction procedures were employed using IRAF¹ (debiasing, flat-fielding, etc.) for pre-processing. Spectra were then extracted at the closest position to the host H II region along the slit (which is ~ 3.7 arcmin in length). Extracted spectra were then wavelength calibrated using standard arc lamps taken before or after each slit position, and flux calibrated using observations of spectrophotometric standard stars taken throughout each night. Spectra were corrected for Galactic extinction using the dust maps of Schlegel, Finkbeiner & Davis (1998) and the standard Galactic reddening law of Cardelli, Clayton & Mathis (1989). Where possible spectra were corrected for extinction internal to the host H II region using the Balmer decrement. However, as stated above, because we are using line diagnostics using the ratio of emission lines close in wavelength, the degree of these corrections (and indeed how accurate the corrections are) should not affect our analysis and derived metallicities, and we therefore believe them to be unimportant.

¹ IRAF is distributed by the National Optical Astronomy Observatories, which are operated by the Association of Universities for Research in Astronomy, Inc., under cooperative agreement with the National Science Foundation.

Table 1. Table listing the SN, host galaxy properties, and observing information for the ISIS subset of the current data sample. In column 1 the SN name is listed followed by the SN type in column 2. In column 3 the SN host galaxy names are listed followed by recession velocities (taken from the NASA/IPAC Extragalactic Database (NED)) then absolute B -band host magnitudes (taken from the Lyon–Meudon Extragalactic DAtabase (LEDA)), Hubble galaxy classifications and T-type galaxy classifications (both taken from the Asiago catalogue). Finally in columns 8 and 9 we list the position angle of the spectrograph slit on the sky and the overall exposure time, which was generally split into three separate exposures to enable cosmic ray removal by median stacking.

SN	Type	Host galaxy	V_r (km s $^{-1}$)	M_B	Hubble type	T-type	Slit PA	Exposure time (s)
1926A	IIL	NGC 4303	1566	−21.82	SBbc	4.2	159	3600
1941A	IIL	NGC 4559	816	−21.11	SBc	6.2	132	3600
1961U	IIL	NGC 3938	809	−20.01	Sc	5.2	242	3600
1962L	Ic	NGC 1073	1208	−19.91	SBc	5.4	166	2700
1964L	Ic	NGC 3938	809	−20.01	Sc	5.2	5	3600
1966J	Ib	NGC 3198	663	−20.48	SBc	5.3	56	3600
1983I	Ic	NGC 4051	700	−19.95	SBbc	4.2	46	3600
1984F	II	UGC 4260	2254	−18.75	Irr	10.0	132	3600
1985F	Ib/c	NGC 4618	544	−19.28	SBd	8.5	41	2700
1985L	IIL	NGC 5033	875	−20.86	Sc	5.0	4	3600
1987M	Ic	NGC 2715	1339	−20.67	SBc	5.1	170	3600
1990H	IIP	NGC 3294	1586	−20.40	Sc	4.9	82	3600
1991N	Ic	NGC 3310	993	−20.04	SBbc	4.0	330	2700
1993G	II	NGC 3690	3121	−20.22	IBm pec	9.0	132	2700
1997X	Ic	NGC 4691	1110	−19.57	SB0/a	0.0	93	2700
1998C	II	UGC 3825	8281	−20.81	Sbc	4.0	176	3600
1998Y	II	NGC 2415	3784	−21.38	Im	10.0	35	2700
1998cc	Ib	NGC 5172	4030	−21.72	Sbc	4.0	101	900
1998T	Ib	NGC 3690	3121	−20.22	IBm pec	9.0	132	2700
1999D	II	NGC 3690	3121	−20.22	IBm pec	9.0	83	2700
1999bw	‘imposter’	NGC 3198	663	−20.48	SBc	5.3	56	3600
1999br	IIP	NGC 4900	960	−19.04	SBc	5.0	107	4500
1999ec	Ib	NGC 2207	2741	−21.50	SBbc	4.3	1	2700
1999ed	II	UGC 3555	4835	−20.48	Sbc	4.0	122	1800
1999em	IIP	NGC 1637	717	−18.45	Sc	5.0	84	3600
1999gn	IIP	NGC 4303	1566	−21.82	SBbc	4.2	159	3600
2000C	Ic	NGC 2415	3784	−21.38	Im	10.0	35	2700
2001B	Ib	IC 391	1556	−19.68	Sc	5.0	3	3600
2001R	IIP	NGC 5172	4030	−21.72	Sbc	4.0	101	900
2001co	Ibc	NGC 5559	5166	−20.66	SBb	3.0	61	2700
2001ef	Ic	IC 381	2476	−20.52	Sbc	3.5	195	2700
2001ej	Ib	UGC 3829	4031	−20.25	Sb	2.7	166	2700
2001gd	Iib	NGC 5033	875	−20.86	Sc	5.0	4	3600
2001is	Ib	NGC 1961	3934	−22.90	Sc	5.0	157	3600
2002ce	II	NGC 2604	2078	−18.89	SBcd	6.0	21	2700
2002ji	Ib/c	NGC 3655	1473	−19.76	Sc	5.0	66	3600
2002jz	Ic	UGC 2984	1543	−18.55	SBdm	8.0	61	3600
2003el	Ic	NGC 5000	5608	−20.84	SBbc	4.0	94	3600
2004bm	Ic	NGC 3437	1283	−19.74	Sc	5.0	136	3600
2004bs	Ib	NGC 3323	5164	−19.70	SBc	5.0	62	3600
2004es	II	UGC 3825	8281	−20.81	Sbc	4.0	176	3600
2004dj	IIP	NGC 2403	131	−19.66	SBc	5.8	126	2700
2004ge	Ic	UGC 3555	4835	−20.48	Sbc	4.0	122	1800
2004gn	Ic	NGC 4527	1736	−21.51	SBbc	3.8	64	3600
2004gq	Ib	NGC 1832	1939	−21.37	SBbc	4.0	56	2700
2005V	Ib/c	NGC 2146	893	−21.10	SBab	2.0	345	3600
2005ay	IIP	NGC 3938	809	−20.01	Sc	5.2	5	3600
2005kk	II	NGC 3323	5164	−19.70	SBc	5.0	62	3600
2005kl	Ic	NGC 4369	1045	−19.00	Sa	1.0	128	2700
2006ov	IIP	NGC 4303	1566	−21.82	SBbc	4.2	159	3600

As mentioned above, many CC SNe do not fall on bright H II regions preventing a metallicity determination at the exact site of each SN detection. However, for all data we already had narrow-band H α imaging, enabling us to centre the slit for spectroscopic observations on the nearest H II region. While this may mean that

for some SNe we do not estimate the ‘true’ progenitor stellar populations metallicity, the estimations that we present should still be more accurate than those published previously either from spectra integrated over whole galaxies or those obtained from more indirect methods as discussed earlier.

Table 2. Table listing the SNIIP and host galaxy properties for the Covarrubias subsample. In column 1 the SN names are listed followed by the host galaxy in column 2. The host galaxy properties recession velocity, absolute B -band magnitude, Hubble type, and finally T-type are given (all sources are the same as in Table 1).

SN	Host galaxy	V_r (km s $^{-1}$)	M_B	Hubble type	T-type
1986L	NGC 1559	1304	−20.40	SBc	5.9
1990E	NGC 1035	1241	−19.03	Sc	5.1
1990K	NGC 150	1584	−20.15	SBb	3.2
1991al	anon	4572			
1992af	PGC 060308	5536	−19.67	Sc	5.0
1992am	PGC 3093690	14310	−20.26	Sa	1.0
1992ba	NGC 2082	1184	−18.17	SBb	3.1
1999ca	NGC 3120	2791	−20.09	Sbc	3.7
1999cr	ESO 576-034	6055	−19.04	Scd	7.1
2000cb	IC 1158	1927	−19.48	Sc	5.0
2002gw	NGC 922	3093	−20.93	SBcd	6.0
2003B	NGC 1097	1271	−21.22	SBb	3.0
2003E	ESO 485-004	4409	−19.70	Sbc	4.3
2003T	UGC 4864	8368	−20.82	Sab	2.0
2003bj	IC 4219	3653	−20.34	SBb pec	3.0
2003ci	UGC 6212	9105	−21.87	Sbc	3.6
2003ef	NGC 4708	4166	−20.35	Sab pec?	2.3
2003fb	UGC 11522	5259	−20.91	Sbc	4.0
2003gd	NGC 628	657	−20.60	Sc	5.0
2003hd	ESO 543-017	11842	−21.82	Sbc	4.2
2003hk	NGC 1085	6789	−21.49	Sbc	3.5
2003hl	NGC 772	2472	−22.75	Sb	3.0
2003hn	NGC 1448	1168	−20.49	Sc	5.9

2.2 Covarrubias sample

The second sample included in this analysis, all of host H II regions of SNIIP (23 in total), presented in Covarrubias (2007) (we have also added an extra SNIIP, 2003gd, that will appear in Covarrubias et al., in preparation), was collected through a range of telescopes/observatories between 2004 and 2006. Spectroscopic data were obtained with the Dual Imaging Spectrograph (DIS) at the APO 3.5-m telescope, Low Dispersion Survey Spectrograph (LDSS)-2 and LDSS-3 on the 6.5-m Clay Telescope, at Las Campanas Observatory (LCO), and the ESO Multi-Mode Instrument (EMMI) on the ESO NTT at La Silla. For details of the instrument setups see Covarrubias et al. (in preparation). As for the ISIS data, prior H α imaging of the SN host galaxies was obtained in order to place the slit on the various instruments on H II regions as close as possible to the position of each SN. All these data were processed and calibrated through standard procedures as above, with emission line fluxes measured in preparation for metallicity estimations. In Table 2, details of the sample are listed.

3 HOST H II REGION METALLICITY DETERMINATIONS

SN host H II region metallicities were derived using the ‘empirical’ methods described in PP04. These authors derive equations relating the ratios of [N II]6583 Å/H α ($N2$) and ([O III]5007 Å/H β)/ $N2$ ($O3N2$), to metallicity, from calibrations using derivations of electron temperatures of H II regions within nearby galaxies. These diagnostics have the advantage (over those such as [N II]/[O II] and the commonly used R_{23} calibrations) of being insensitive to extinction due to the small separation in wavelength of the emission lines used for the ratio diagnostics. We also employ these diagnostics as

they will be insensitive to differential refraction, which is particularly pertinent for the ISIS data, as many of these spectra were not taken at the parallactic angle, as discussed above. For all H II regions within our sample, we therefore derive oxygen abundances using the $N2$ and where possible (in some cases we did not detect the oxygen or H β emission lines), the more accurate $O3N2$ line ratios. These values are listed in Table 3. PP04 note that their calibration fit is only valid for $O3N2 < 1.9$. There is one case in our sample where this condition was not met (for the environment of SN 1999cr), and we therefore use the $N2$ ratio instead. We also note that above solar metallicity ($12 + \log(O/H) = 8.66$; Allende Prieto, Lambert & Asplund 2001; Asplund et al. 2004) [N II] tends to saturate (Baldwin, Phillips & Terlevich 1981) making $N2$ an unreliable metallicity indicator. There are 11 of these cases in the current sample, where we only detect H α and [N II], made up of six SNIbc and five SNII. While these derived metallicities are probably somewhat in error we are unable to derive more accurate values. We do not think they will heavily influence the overall results presented below, and we therefore include them in the analysis but note them with a star in Table 3 ([N II] fluxes are also present in the $O3N2$ diagnostic, however the effects of its saturation will be diluted by the presence of other lines in the estimation, and therefore it is thought that $O3N2$ will still be reliable above solar values).

In the last column of Table 3 we list the distance between the catalogued SN position (taken from the Asiago catalogue or derived from our own images in the case of the Covarrubias sample) and the position of the extracted spectrum used to determine the progenitor metallicity. This distance is calculated from the difference between the deprojected galactocentric radius of the SN position and that of the H II region where the spectrum was extracted. If these two positions are identical (i.e. the SN fell on a bright H II region), this distance is listed as ‘SN’. In Section 5.1, we analyse whether including those measurements at considerable distances from the SN position may affect our results and conclusions. Next we present the results from the above derived CC SN progenitor metallicities.

4 RESULTS

4.1 Type II supernovae

The mean oxygen abundance for the 46 SNII in the current sample, on the PP04 scale, is 8.580 with a standard error on the mean of 0.027. This sample spans ~ 0.75 dex in metallicity, with SNII occurring in significant numbers at both high and low metallicity. This sample is dominated by SNIIP (67 per cent), the mean metallicity for this subset being 8.587 (0.034). In the sample of SNII there are also four SNIIL, which have a mean metallicity of 8.520 (0.028), thus lower than the SNIIP. Although with only four objects, any difference between these types is not statistically significant. There is also one SNIIB (thought to be transitional objects between SNII and SNIb) in the current sample having an $N2$ metallicity of $8.60^{+0.23}_{-0.22}$. Finally there is also one SN ‘imposter’ in the sample, 1999bw (which we do not include in the SNII sample), and this has an $N2$ metallicity of $8.50^{+0.30}_{-0.28}$.

4.2 Type Ibc supernovae

The 10 SNIb in the sample have a mean abundance of 8.616 (0.040), while the 14 SNIc have a mean of 8.626 (0.039). Combining both the above samples, the mean metallicity for the 27 SNIbc (adding an additional three SNe that only have Ib/c classification, note that

Table 3. CC SN progenitor metallicities derived from host H II regions. In the first column, the SN name is listed followed by the SN type. Then the $N2$ metallicity is given together with errors, followed by the $O3N2$ metallicity together with its associated errors. These errors are a combination of flux calibration errors, statistical errors estimated from the variation of the continuum close to the measured line fluxes, and the 1σ spread in the calibration of each line diagnostic taken from PP04. In most cases, this last calibration error dominates. In the final column, the distances between the galactocentric radial SN position and that of the H II regions used for the metallicity derivation are listed. If these positions are the same then those cases are listed as ‘SN’. Those SNe marked with a star (*) refer to where the metallicity determination may be somewhat in error due to the saturation of the [N II] line (see text for further details).

SN	Type	$N2$	$O3N2$	Distance from SN position (kpc)
1926A	IIL	$8.66^{+0.21}_{-0.21}$	$8.50^{+0.13}_{-0.13}$	2.23
1941A	IIL	$8.54^{+0.21}_{-0.21}$		SN
1961U	IIL	$8.47^{+0.21}_{-0.21}$	$8.47^{+0.13}_{-0.13}$	0.75
1962L	Ic	$8.36^{+0.23}_{-0.22}$	$8.33^{+0.14}_{-0.14}$	6.92
1964L	Ic	$8.59^{+0.21}_{-0.21}$		0.28
1966J	Ib	$8.57^{+0.23}_{-0.23}$		0.39
1983I*	Ic	$8.73^{+0.21}_{-0.21}$		2.37
1984F	II	$8.14^{+0.21}_{-0.21}$	$8.13^{+0.13}_{-0.13}$	0.86
1985F	Ib	$8.43^{+0.21}_{-0.21}$		SN
1985L	IIL	$8.59^{+0.22}_{-0.22}$	$8.60^{+0.14}_{-0.14}$	2.17
1986L	IIP	$8.52^{+0.21}_{-0.21}$	$8.51^{+0.13}_{-0.13}$	0.74
1987M	Ic	$8.65^{+0.21}_{-0.21}$		0.03
1990E	IIP	$8.57^{+0.21}_{-0.21}$		2.99
1990H	IIP	$8.68^{+0.21}_{-0.21}$		SN
1990K	IIP	$8.63^{+0.21}_{-0.21}$	$8.63^{+0.13}_{-0.13}$	0.57
1991N	Ic	$8.49^{+0.21}_{-0.21}$	$8.44^{+0.13}_{-0.13}$	SN
1991al	IIP	$8.47^{+0.21}_{-0.21}$	$8.61^{+0.13}_{-0.13}$	3.39
1992af	IIP	$8.37^{+0.21}_{-0.21}$	$8.36^{+0.13}_{-0.13}$	0.38
1992am	IIP	$8.66^{+0.21}_{-0.21}$	$8.69^{+0.13}_{-0.13}$	14.53
1992ba	IIP	$8.52^{+0.21}_{-0.21}$	$8.66^{+0.13}_{-0.13}$	0.42
1993G	IIL	$8.56^{+0.21}_{-0.21}$	$8.51^{+0.13}_{-0.13}$	SN
1997X	Ic	$8.65^{+0.21}_{-0.21}$	$8.68^{+0.13}_{-0.13}$	SN
1998C*	II	$8.86^{+0.23}_{-0.23}$		SN
1998T	Ib	$8.60^{+0.21}_{-0.21}$	$8.53^{+0.13}_{-0.13}$	SN
1998Y	II	$8.62^{+0.21}_{-0.21}$	$8.61^{+0.13}_{-0.13}$	SN
1998cc	Ib	$8.82^{+0.23}_{-0.23}$		1.33
1999D	II	$8.75^{+0.21}_{-0.21}$	$8.56^{+0.13}_{-0.13}$	2.64
1999br	IIP	$8.52^{+0.21}_{-0.21}$		0.35
1999bw	‘imposter’	$8.50^{+0.30}_{-0.28}$		0.92
1999ca	IIP	$8.45^{+0.21}_{-0.21}$	$8.45^{+0.13}_{-0.13}$	0.43
1999cr	IIP	$8.11^{+0.21}_{-0.21}$		6.11
1999ec	Ib	$8.44^{+0.26}_{-0.25}$	$8.45^{+0.15}_{-0.15}$	0.10
1999ed	II	$8.79^{+0.21}_{-0.21}$	$8.78^{+0.13}_{-0.13}$	SN
1999em	IIP	$8.61^{+0.23}_{-0.23}$		0.23
1999gn*	IIP	$8.87^{+0.24}_{-0.23}$		SN
2000C	Ic	$8.62^{+0.21}_{-0.21}$	$8.61^{+0.13}_{-0.13}$	SN
2000cb	IIP	$8.53^{+0.21}_{-0.21}$	$8.70^{+0.13}_{-0.13}$	3.68
2001B	Ib	$8.66^{+0.21}_{-0.21}$	$8.55^{+0.13}_{-0.13}$	SN
2001R*	IIP	$8.80^{+0.24}_{-0.23}$		4.38
2001co*	Ib/c	$8.70^{+0.21}_{-0.21}$		3.01
2001ef*	Ic	$8.84^{+0.23}_{-0.23}$		SN

Table 3 – continued

SN	Type	$N2$	$O3N2$	Distance from SN position (kpc)
2001ej	Ib	$8.77^{+0.22}_{-0.21}$	$8.74^{+0.13}_{-0.13}$	SN
2001is	Ib	$8.67^{+0.23}_{-0.22}$	$8.58^{+0.13}_{-0.13}$	1.47
2001gd	Ib	$8.60^{+0.23}_{-0.22}$		0.30
2002ce	II	$8.49^{+0.13}_{-0.13}$	$8.51^{+0.13}_{-0.13}$	0.07
2002gw	IIP	$8.24^{+0.21}_{-0.21}$	$8.27^{+0.13}_{-0.13}$	0.81
2002ji	Ib/c	$8.64^{+0.22}_{-0.22}$	$8.74^{+0.13}_{-0.13}$	0.56
2002jz	Ic	$8.12^{+0.21}_{-0.21}$	$8.38^{+0.14}_{-0.13}$	0.35
2003B	IIP	$8.73^{+0.21}_{-0.21}$	$8.79^{+0.13}_{-0.13}$	3.80
2003E	IIP	$8.14^{+0.21}_{-0.21}$	$8.23^{+0.13}_{-0.13}$	0.28
2003T	IIP	$8.64^{+0.21}_{-0.21}$	$8.66^{+0.13}_{-0.13}$	2.29
2003bj	IIP	$8.64^{+0.21}_{-0.21}$	$8.77^{+0.13}_{-0.13}$	0.07
2003ci	IIP	$8.61^{+0.21}_{-0.21}$	$8.77^{+0.13}_{-0.13}$	5.18
2003el*	Ic	$8.67^{+0.24}_{-0.23}$		0.04
2003ef	IIP	$8.66^{+0.21}_{-0.21}$	$8.81^{+0.13}_{-0.13}$	1.62
2003ie*	II	$8.88^{+0.24}_{-0.23}$		1.18
2003fb	IIP	$8.58^{+0.21}_{-0.21}$	$8.63^{+0.13}_{-0.13}$	4.52
2003gd	IIP	$8.54^{+0.21}_{-0.23}$	$8.61^{+0.15}_{-0.15}$	0.20
2003hd	IIP	$8.52^{+0.21}_{-0.21}$	$8.50^{+0.13}_{-0.13}$	1.31
2003hk	IIP	$8.62^{+0.21}_{-0.21}$	$8.60^{+0.13}_{-0.13}$	13.43
2003hl	IIP	$8.66^{+0.21}_{-0.21}$	$8.87^{+0.13}_{-0.13}$	1.00
2003hn	IIP	$8.46^{+0.21}_{-0.21}$	$8.46^{+0.13}_{-0.13}$	3.30
2004bm	Ic	$8.63^{+0.21}_{-0.21}$	$8.70^{+0.13}_{-0.13}$	SN
2004bs	Ib	$8.62^{+0.21}_{-0.21}$	$8.71^{+0.13}_{-0.13}$	SN
2004dj	IIP	$8.31^{+0.21}_{-0.21}$		0.33
2004es	II	$8.44^{+0.22}_{-0.22}$		SN
2004ge*	Ic	$8.71^{+0.21}_{-0.21}$		SN
2004gq	Ib	$8.72^{+0.21}_{-0.21}$	$8.75^{+0.13}_{-0.13}$	0.15
2004gn	Ic	$8.66^{+0.21}_{-0.21}$		SN
2005V	Ib/c	$8.83^{+0.21}_{-0.21}$	$8.76^{+0.13}_{-0.13}$	SN
2005ay*	IIP	$8.66^{+0.23}_{-0.23}$		SN
2005kl	Ic	$8.62^{+0.21}_{-0.21}$	$8.74^{+0.13}_{-0.13}$	SN
2005kk	II	$8.45^{+0.21}_{-0.21}$	$8.48^{+0.13}_{-0.13}$	SN
2006ov	IIP	$8.66^{+0.21}_{-0.21}$	$8.50^{+0.13}_{-0.13}$	0.68

all these metallicities are reasonably high, hence the higher value of this mean than both that of the Ib and Ic samples) is 8.635 (0.026). We therefore find that while in terms of mean metallicity values the SNIbc seem to arise from more metal rich environments, and hence progenitors than SNII, this difference is only marginal.

This is shown in Fig. 1, where we plot the derived host H II region metallicities for the SNII (black squares) and SNIbc (red triangles) against host galaxy absolute B -band magnitude, which should be a rough proxy for global galaxy metallicity. While there is much scatter in the plot, one can see that overall the SNIbc appear to have slightly higher derived metallicities than the SNII. In particular, the lowest five metallicities are derived from SNII host H II regions (although, also note that, the *highest* three metallicities are also derived from SNII host H II regions). While there appears to be a difference in metallicity between the two progenitor populations, this difference is not hugely significant. In terms of the means of the populations, there is only 0.06 dex (at a level of $\sim 1.5\sigma$) difference in progenitor metallicities. Using a Kolmogorov–Smirnov (KS) test,

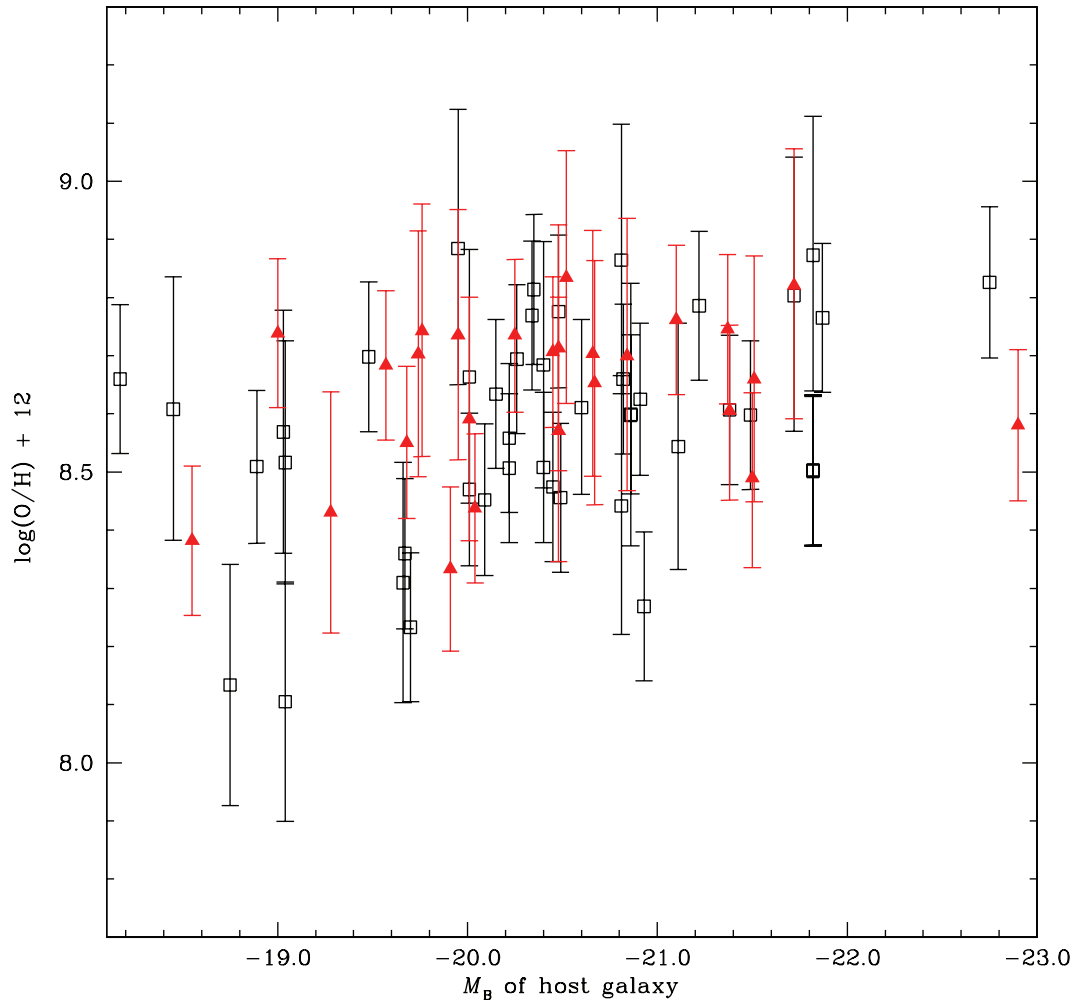


Figure 1. Derived PP04 oxygen metallicities for CC SN host H II regions against absolute B -band magnitudes of host galaxies. SNI are plotted in black squares and the overall SNIbc population are plotted in red triangles.

again the difference between the two populations is only marginal, with ~ 16 per cent chance that the two distributions are drawn from the same parent population.

In Fig. 2 we show a similar plot but split the SNIbc into individual classes. The SNI are shown in black squares, the SNIb in blue triangles, the SNIc in red triangles and finally those with only Ib/c classification are shown in green triangles. Any differences in derived metallicity between these individual classes are hard to see directly from this plot. However, in terms of the mean values for each class, there is a suggestion of a metallicity sequence in terms of the SNI arising from the lowest metallicity progenitors, followed by the SNIb and finally the SNIc arising from the highest metallicity environments and hence progenitors. It is also interesting to note that there appears to be more of a spread in metallicity for the SNIc compared to the SNIb, something that is shown in their deviations from the mean, with the SNIc showing a 1σ spread of 0.145 dex compared to 0.128 for the SNIb.

In terms of overall host galaxy absolute B -band magnitude, which should correlate with overall galaxy metallicity, any differences between the SNIbc and SNI hosts are even less apparent than for derived environment metallicities. The mean absolute B -band magnitude for the SNI hosts is -20.42 compared to -20.43 for the SNIbc hosts. Hence in terms of host galaxy magnitude, the two

distributions are completely consistent with each other (which is confirmed by application of the KS test). Therefore, on both a local and global scale we do not find conclusive evidence that the overall progenitor metallicities of SNIbc are significantly higher than those of SNI.

5 DISCUSSION

The results presented above show that the difference in mean metallicity between the SN types is low, and statistically at best marginal. The simplest interpretation of this result is therefore that while progenitor metallicity probably plays some role in deciding SN type (through increasing the pre-SN mass loss through line-driven winds and hence stripping the progenitor star of additional amounts of its envelope), its role is likely to be small compared to that played by initial progenitor mass and the role of binary companions to the progenitor star. These statistical differences in progenitor metallicity are again illustrated in Fig. 3. Here we plot the cumulative distribution of progenitor metallicities for the SNI (black), the SNIb (dashed blue), the SNIc (dashed red) and the overall SNIbc population (green). We see that while, as discussed, the difference between the SNI and SNIbc distributions is not huge, there does seem to be an offset between the metallicity of the two populations. This

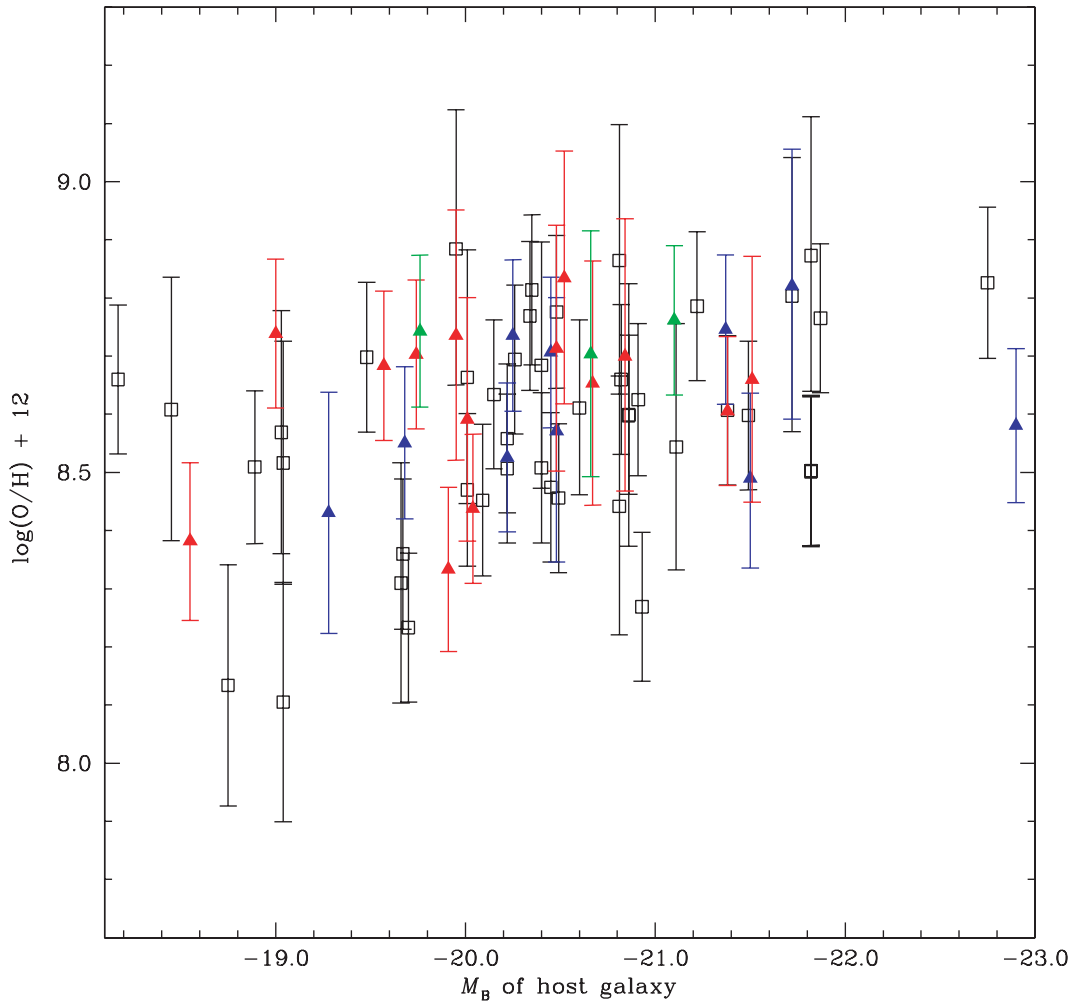


Figure 2. Derived PP04 oxygen metallicities for CC SN host H II regions against absolute B -band magnitudes of host galaxies. Here we split the SNIbc into individual classes. SNIa are plotted in black squares, SNIb in blue triangles, SNIc in red triangles and finally those only classified as SNIb/c are plotted in green triangles.

plot also emphasizes the low significance of any statistical difference between the SNIb and SNIc populations. It is also interesting to note that at low metallicities ($< \sim 8.3$) the CC SN distribution exclusively produces SNIa in the current sample.

The interpretation that progenitor mass plays a significantly larger role in determining SN type is backed up by previous work using pixel statistics from host galaxy H α imaging of CC SN host galaxies (AJ08), investigating the association of different SN types with recent SF. It was found with high statistical significance that SNIbc showed a higher degree of association to the H α emission of their host galaxies than SNIa. The most logical explanation for this result is that the stellar lifetimes are significantly shorter for SNIbc than SNIa, which implies higher mass progenitors for the former. In a separate publication (AJ09), it was found that SNIbc were more centrally concentrated than SNIa (with respect to both the old stellar continuum traced by R -band light and the young stellar host galaxy component traced by H α emission), the initial interpretation being that this implied a significant progenitor metallicity difference between the two classes. Indeed, it was found that the SNe coming from the central 20 per cent of the host galaxies' light were completely dominated by SNIbc and in particular SNIc, implying that at high metallicities the CC SN progenitor channel highly favoured

the production of these types. However, this trend is not seen in the current work. Here we find that SNIa are produced in significant numbers at all metallicities, with the highest three derived host H II region metallicities being for this SN type. AJ09 also found a lack of SNIc at large galactocentric radii implying that these SNe require high-metallicity environments to achieve the required envelope stripping to explode as SNIc. Again, however, we do not see this in the current work with a number of SNIc having relatively low derived metallicities. Indeed there are now other examples in the literature (see further analysis and discussion in Section 5.5), of SNIc arising from low-metallicity environments. These two works therefore seem somewhat in contradiction. However, as discussed earlier, recent further analysis of the AJ09 sample (HAJ10), splitting the sample into disturbed and undisturbed host galaxies now indicates that this initial assumption of centralization of events being caused solely by metallicity differences may have been too simplistic. It was found that this centralization of SNIbc events is much more pronounced in galaxies showing signs of disturbance or interaction. This trend is difficult to explain in terms of metallicity effects as one would expect metallicity trends to be smaller or non-existent in galaxies undergoing some kind of merging event where the flow of unenriched gas to the centres of galaxies is likely to lower central

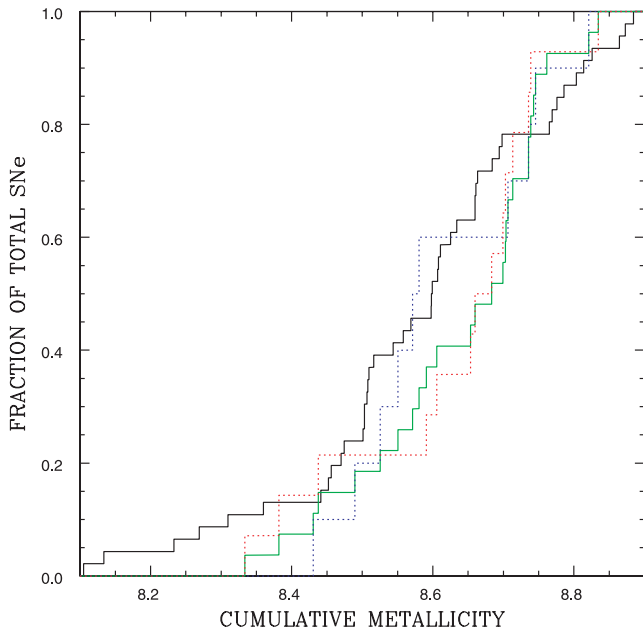


Figure 3. Plot showing the cumulative distribution of the metallicities of the local gas-phase environments of the different SN types. The SNII population is shown in solid black, the SNIb population in dashed blue, the SNIc population in dashed red and the overall SNIbc population in solid green.

metallicities. This work claims that the most logical explanation is that this shows evidence for a shallower high-mass IMF in the central parts of disturbed galaxies, and hence an increased production of SNIbc over SNII. These results therefore very much complicate the interpretations that can be made from differences in the positions of different SN types found within host galaxies. Additional work needs to be employed to differentiate between the possible effects of changes in environment metallicity and IMF, and indeed for more reliable progenitor metallicity studies methods such as those employed here are needed.

Together with the work of Modjaz et al. (2008) (further discussed below) the most related recent study to that presented here is that of Prieto et al. (2008). As discussed earlier, these authors used ‘global’ gas-phase metallicities derived for SDSS galaxies host to SNe to investigate differences between progenitor metallicities of different SN types. It is therefore interesting to compare the two studies. Prieto et al. (2008) used a sample of 58 SNII and 19 SNIbc that had occurred in SDSS host galaxies where spectral observations had been taken. These authors found a difference between the mean abundances of SNII and SNIbc of 0.12 dex, twice as large as the difference found here. This may seem slightly surprising as their analysis was of ‘global’ metallicities and hence does not take into account gradients within galaxies (as we assume our analyses should). Given that these are then likely to overestimate the metallicity of SNII with respect to SNIb/c (because of the differences between the radial distributions of the two types; although see Section 5.4), one would actually expect that there would be a *larger* difference in mean metallicities in the current sample. These results are therefore slightly puzzling, however we put these differences down to the still relatively small sample sizes of each study and therefore the relatively low statistical significance ($\sim 1.5\sigma$ here and $\sim 2\sigma$ in Prieto et al. 2008) of these metallicity differences.

5.1 ‘Local’ and ‘nearby’ host H II regions

As we discussed earlier, many SNII do not fall on bright H II regions within galaxies. While SNIbc generally show a higher degree of association to host galaxy H α emission, even these do not always fall directly on large bright H II regions where one can be confident of detecting the emission lines needed for metallicity determinations with adequate signal to noise ratio. During the observational stage of this project, this fact was overcome by using narrow-band H α imaging already in hand to locate the closest H II regions to the catalogued SN positions, in order to place the slit of the various spectrographs employed on the desired region of the host galaxy. It is obvious however that this technique may adversely affect the results as metallicities may be determined for SN progenitors that do not reflect the ‘true’ metallicity of the environment local to the original SN position at the epoch of SF. Here we investigate if any such effect is at play in the above results by splitting the sample into ‘local’ (i.e. at or very nearby to the SN explosion coordinates) and ‘nearby’ (i.e. where the extraction of the spectrum used for the metallicity determinations is significantly far away from the SN position) samples.

To make this separation we assume a delay time for CC SNe (time between SF epoch and SN explosion) of 20 Myr, and a typical progenitor velocity of 30 km s^{-1} (stars with velocities much higher than this are generally considered special cases and are classified as ‘runaways’; Blaauw 1961). This leads to a typical distance travelled by a CC SN progenitor before explosion epoch of $\sim 600 \text{ pc}$. Therefore an accurate local metallicity should be considered, any that is derived within this distance from the catalogued SN position. We therefore split the current sample into those inside and outside this limit using the values presented in Table 3. We then recalculate the mean values for the SNII and SNIbc for both the ‘local’ and ‘nearby’ samples. As expected the fraction of SNIbc (81 per cent) within this distance limit is substantially higher than for SNII (49 per cent), as SNIbc are generally found significantly closer to bright H II regions (AJ08). The mean metallicities for SNII where the derivation was achieved within 600 pc of the SN position is 8.570, compared to 8.581 for those outside. For the SNIbc, the five metallicity determinations further than 600 pc have exactly the same mean metallicity for those ‘local’ to the SN. These results mean that we can confidently include those metallicity determinations (38 per cent) that are taken away from the explosion site of the sample SNe. While these metallicities will likely be slightly different from those at the exact site of the individual SNe, the above analysis shows that they are unlikely to bias the results in one particular direction.

5.2 Host galaxy properties and possible biases

One may ask whether the sample of SNe and their host galaxies included in the current analysis are a true representation of that occurring in nature. These SNe were found from a large number of different search programs (both amateur and professional), all of which have different search parameters. It is therefore impossible to study any subset which is in any way unbiased. However, we can study the host galaxy properties to understand how different the current sample may be from that in nature. The main inadequacy of many SN searches to date is their galaxy targeted nature and the higher degree of time spent looking at massive nearby galaxies where one can hope to increase the likelihood of SN detection. This in general means that smaller, lower metallicity galaxies may be underrepresented in SN catalogues. However, we note that James & Anderson (2006) investigated this effect and found that there

was no large bias present when looking at where within the overall sample of the H α Galaxy Survey (James et al. 2004) SNe had been discovered, with respect to the SF rate of the sample galaxies. Non-galaxy targeted searches are starting to find a small number of events in unclassified very small galaxies (see e.g. Arcavi et al. 2010 for examples of these types of SN discoveries in ‘rolling’ searches). However, the contribution of these events to the overall SN rates is likely to be very small due to the very low SF rates that these galaxies will have. Hence this possible bias of using SNe discovered from galaxy targeted for overall sample studies is probably very low, if existent at all.

In Section 2 we stated that we assumed that the current sample is a random selection of targets taken from AJ09. While this is true, the low numbers of events may mean we are unwittingly using a subset that is different in host galaxy properties (and therefore may be producing different SNe), than the original parent sample. To test this we use the host galaxy T-types as listed in Tables 1 and 2, to calculate a mean T-type of 4.79 with a standard error on the mean of 0.23 for the current sample. We can then compare this to the larger sample from AJ09 which has a mean host galaxy T-type of 4.55 (0.15) and hence within the errors the subsample presented here is consistent with the overall parent sample. We believe that this comparison is valid because the AJ09 sample was a large fraction of the catalogued SNe occurring within $\sim 6000 \text{ km s}^{-1}$ and therefore both that sample, and because of the above analysis the current sample, are a random sample of the *observed* SNe to date. We acknowledge that there are probably certain ‘special’ case SNe lacking from our sample, but given the low SF rates of their likely hosts their rates are likely low and will therefore not have a huge impact on studies of the type presented here.

Above we have discussed the results of HAJ10, where a dependence of SN radial position (within host galaxies) on the disturbance of the host galaxy was found. This correlation has been interpreted as evidence of a different IMF in the nuclear SF regions of these galaxies, where more SNIbc are produced at the expense of SNII. Therefore another source of possible bias in the current sample is whether there are more/less cases of host galaxy disturbance than found in other samples. In HAJ10 (where basically the same sample as AJ09 with a small number of extra data included was used) 33 per cent of CC SNe were found in disturbed galaxies, with the other 67 per cent found in undisturbed systems (all classifications were done visually). In the current sample these values change to 40 per cent (disturbed) and 60 per cent (undisturbed). Hence there are more SNe found in systems where changes in IMF may also be affecting the relative number of SNII to SNIb/c together with progenitor metallicity. While these differences in host galaxies are only small they may affect the current results in reducing the impact of progenitor metallicity and increasing the impact of a changing IMF on producing the correlations of CC SNe types on progenitor environment. Therefore we note this as a small caveat to the results and conclusions presented here.

5.3 Comparison to stellar models

Single star models (e.g. Heger et al. 2003; Eldridge & Tout 2004; Meynet & Maeder 2005) generally predict that the production rate of SNIbc relative to SNII is correlated with progenitor metallicity. Heger et al. (2003) concluded that SNIbc production required supersolar metallicities and that therefore they were not produced in significant numbers by single star progenitors. However, their models lacked rotation, the inclusion of which by different authors (Meynet & Maeder 2005) significantly lowered the required metal-

licity for SNIbc production. Georgy et al. (2009) compared the observed ratio of SNII to SNIbc with both their single star models with rotation and the binary models of Eldridge, Izzard & Tout (2008). While this seems a worthwhile pursuit in gaining knowledge of progenitor characteristics, the current statistics of the CC SN ratio at different metallicities means that differentiating between stellar models (the binary models of Eldridge et al. 2008 also predict the overall observed trends of increasing SNIbc to SNII ratio with metallicity) is difficult due to the relatively small differences between the model predictions and the currently small number of SNe with metallicity estimations (especially when binning the SNIbc/II ratio into several metallicity subsets). We therefore refrain from comparing our results to progenitor models until we have obtained sufficient statistics to differentiate between different model predictions. It is also unclear how to directly compare absolute metallicities between the different observational studies (such as Prieto et al. 2008) as the use of different line diagnostics with significant offsets in calibrated metallicities make comparing like with like extremely difficult. Given the relatively large offsets between different line diagnostic methods, any comparison on absolute metallicities is perhaps premature. While we quote our absolute mean metallicities derived for the sample presented here, our main results do not rely on these values. The results presented in this paper are most significant in terms of relative *differences* in metallicity.

5.4 Analysis of Boissier & Prantzos (2009)

Boissier & Prantzos (2009) (hereafter BP09) recently published results on the progenitor metallicities of different CC SN types through a study of the estimated local environment metallicity derived from global galaxy luminosities and assumed metallicity gradients. These authors calculated progenitor metallicities in this way for a large sample of SN host galaxies taken from the Asiago SN catalogue. Given that in our current sample we have *directly* derived ‘local’ metallicities for SN progenitors, we are in a position to test these more indirect methods.

For SNe in the current sample, we derived a ‘local’ metallicity using equation (6) from BP09 and follow these authors in taking absolute host *B*-band magnitudes from the LEDA data base and the R_{25} radius from the Asiago catalogue. We can then compare these metallicities with those derived from host H II region spectra as presented here.

Overall we find an offset between the two methods of deriving metallicities of ~ 0.35 dex, in terms of the BP09 metallicities being higher than those derived here. However, this is unsurprising as their calibration uses the mass–metallicity relationship from Garnett (2002), where different diagnostics were used to those employed here. It is known that the ‘empirical’ methods we employ here give systematically lower metallicities than those derived from, for example, photoionization models (e.g. Kewley & Dopita 2002). While the origin of these differences is still debated, as long as *all* metallicity derivations are offset between different diagnostics then their use for the current study is justified where the main aim is to search for *differences* between different SN types. Therefore, in comparing our metallicities with those determined using the BP09 technique, what is of more interest is the spread of these offsets. We find a 1σ standard deviation around this mean offset of ~ 0.19 dex. Calculating the mean error on our metallicity determinations listed in Table 3 (all 1σ errors), we obtain a value of 0.16 dex. Hence the spread of the differences between these two methods is only slightly larger than one would expect from the errors we estimate here from our ‘direct’ abundance measurements. We therefore conclude that

the BP09 technique overall gives reasonable estimates for environment metallicities which are adequate for large population scale studies. However for more precise measurements, especially when comparing small SN samples, we encourage more observations and derived metallicities from spectra obtained close to SN explosion positions.

The above analysis was performed to check the overall accuracy of the BP09 technique compared to that employed here, irrespective of SN type. Now we use the BP09 method to calculate mean values for the SNIbc and SNII distributions in the current sample. Using their method we calculate a mean metallicity of 8.91 for 46 SNII and 9.02 for 27 SNIbc, and we find a 0.1 dex metallicity difference between the two distributions. Furthermore using a KS test we find only a 2.3 per cent chance that the two distributions are drawn from the same parent population. Hence these results seem in contradiction to those from the current study where only a marginal metallicity difference between the two SN types was found. We speculate that this difference is related to the radial distribution of the two SN types within their host galaxies, and how much these radial trends are related to progenitor metallicity. As discussed in detail earlier, the results of HAJ10 suggest that (at least in that sample) the overall centralization of SNIbc in host galaxies is driven (almost entirely) by SNe in galaxies that show signs of disturbance. Those galaxies showing signs of disturbance/evidence of interaction with a merging companion are likely to have much flatter (or even non-existent) metallicity gradients than their undisturbed counterparts. Hence when the radial term in equation (6) from BP09 is used it *may* often be overestimating the metallicity for those SNIbc found in the central parts of galaxies. We can investigate this assertion using the above analysis. When splitting the SNe into SNII and SNIbc, we find that the offset between our metallicity estimations and those using the BP09 method is indeed greater for

SNIb/c (we find an offset for SNII of 0.34 dex and 0.38 dex for the SNIbc), and the BP09 method seems to overestimate environment metallicities for SNIb/c, at least those in the current sample. The SNIbc used in this work are closer to the centres of their host galaxies than the SNII (having a mean R/R_{25} of 0.30 compared to 0.47 for the SNII), as observed in AJ09 and other previous studies, and therefore BP09 will correct the metallicities for this trend, even though the correlation of SN type with radial position may not be determined by metallicity. This may therefore be the source of the discrepancy.

5.5 Literature progenitor metallicities

While the current study is (to our knowledge) the first to publish a large sample of environment metallicities for the main CC SN types, over the last few years a number of individual progenitor metallicities have been published by various authors, along with the GRB/SNIc sample published by Modjaz et al. (2008). In this section we therefore bring all these metallicities together and discuss their overall implications for CC progenitor metallicities and on future SN environment studies. These literature metallicities are listed in Table 4 together with their references.

In Fig. 4, we reproduce Fig. 2 but add those progenitor metallicities from Table 4. The first observation that can be made from this plot is that the four lowest metallicities are those for GRB environments. This observation, that GRBs in general favour lower metallicity environments than SNIc without accompanying GRBs, was the major conclusion from Modjaz et al. (2008). While we do not add to the statistics on SNIc broad line or GRB metallicities here, the current work supports this view that *generally* (although we note the case of GRB 020819) when compared to all SN types GRBs favour lower metallicity environments. We also see a

Table 4. Table listing the CC SN and GRB environment metallicities (on the PP04 scale) found through a search of the current literature. In the first column the SN/GRB names are listed. This is followed by the host galaxy name and absolute B -band magnitude. Finally, the environment metallicity together with its associated error are listed followed by the reference for these data in the final column.

SN/GRB	Type	Host galaxy	Galaxy M_B	Metallicity	Reference
1997ef	Ic BL	UGC 4107	-19.97	$8.69^{+0.13}_{-0.13}$	Modjaz et al. (2008)
1998ey	Ic BL	NGC 7080	-21.78	$8.72^{+0.14}_{-0.14}$	Modjaz et al. (2008)
1999eh	Ib	NGC 2770	-20.74	$8.50^{+0.21}_{-0.21}$	Thöne et al. (2009)
GRB020819	GRB	anon		$8.70^{+0.13}_{-0.14}$	Levesque et al. (2010b)
GRB020903	GRB	anon	-18.80	$8.00^{+0.10}_{-0.10}$	Modjaz et al. (2008)
GRB030329/2003dh	GRB/SNIc BL	anon	-16.50	$7.50^{+0.10}_{-0.10}$	Modjaz et al. (2008)
2003jd	Ic BL	MCG -01-59-21	-19.77	$8.39^{+0.13}_{-0.13}$	Modjaz et al. (2008)
GRB031203/2003lw	GRB/SNIc BL	anon	-21.00	$7.80^{+0.10}_{-0.10}$	Modjaz et al. (2008)
2005kr	Ic BL	J030829.66+005320.1	-17.40	$8.24^{+0.13}_{-0.13}$	Modjaz et al. (2008)
2005ks	Ic BL	J213756.52-000157.7	-19.20	$8.63^{+0.13}_{-0.13}$	Modjaz et al. (2008)
2005nb	Ic BL	UGC 7230	-21.30	$8.49^{+0.13}_{-0.13}$	Modjaz et al. (2008)
GRB/XRF060218/2006aj	GRB/XRF/SNIc BL	anon	-15.90	$7.50^{+0.10}_{-0.10}$	Modjaz et al. (2008)
2006nx	Ic BL	J033330.43-004038.0	-18.90	$8.24^{+0.13}_{-0.13}$	Modjaz et al. (2008)
2006qk	Ic BL	J222532.38+000914.9	-21.00	$8.75^{+0.13}_{-0.13}$	Modjaz et al. (2008)
2007I	Ic BL	J115913.13-013616.1	-16.90	$8.39^{+0.42}_{-0.21}$	Modjaz et al. (2008)
2007bg	Ic BL	anon	-12.40	$8.18^{+0.17}_{-0.17}$	Young et al. (2010)
2007uy	Ib	NGC 2770	-20.74	$8.50^{+0.13}_{-0.13}$	Thöne et al. (2009)
2007ru	Ic BL	UGC 12381	-20.34	$8.78^{+0.13}_{-0.13}$	Sahu et al. (2009)
2008D	Ib	NGC 2770	-20.74	$8.60^{+0.21}_{-0.21}$	Tanaka et al. (2009), Thöne et al. (2009)
2009bb	Ic BL	NGC 3278	-19.98	$8.68^{+0.13}_{-0.13}$	Levesque et al. (2010a)

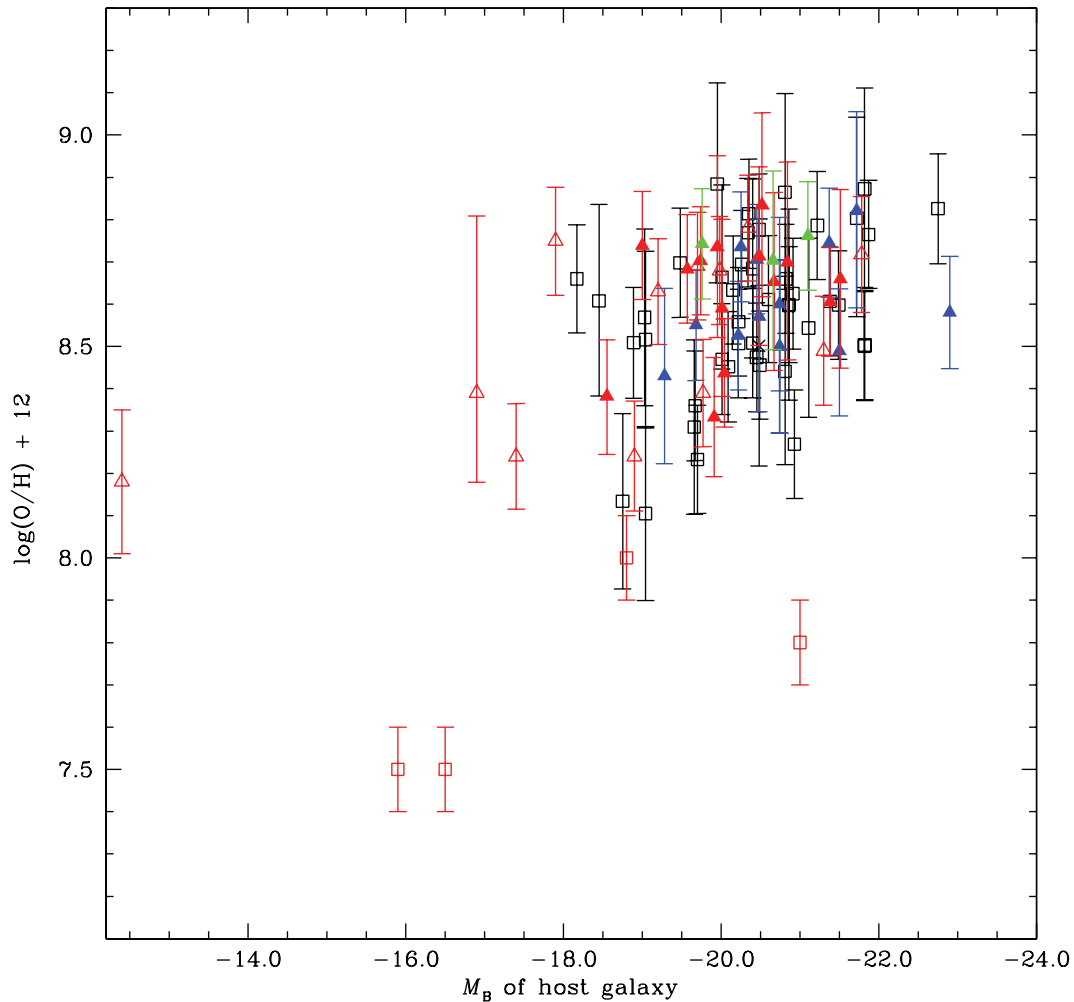


Figure 4. Same as Fig. 2 except here we include all literature metallicities as listed in Table 4. Here the SNIa are shown in black squares, SNIb in blue filled triangles, SNIc in red filled triangles, SNIc broad line in red open triangles and SNIc broad line with associated GRBs in red open squares. Note that the quoted errors are a combination of the diagnostic calibration error, and the flux calibration and statistical errors as taken from the relevant reference.

number of broad-line SNIc at low metallicities with four exploding in the lowest luminosity host galaxies. While this is interesting it is probably unwise to draw firm conclusions from this observation, as many of these events have published data *because* they are interesting cases (i.e. associated with GRBs, occurring in strange environments), and therefore it is possible that their rates when compared to other objects on the plot may be unrealistic.

It is clear from the above results and discussion that investigating progenitor metallicity differences between different SN types is complicated, due to the absence of unbiased samples, and the uncertain nature of other factors that play a role in defining SN types from environmental conditions. Eventually when untargated SN searches catch up in terms of nearby SN discoveries, we will be able to reduce these biases and attempt to constrain the true range of environments which different SN types are found in and their relative rates. For now we must continue to increase the sample sizes such as those presented here, in order to gain further knowledge of SN progenitor characteristics.

6 CONCLUSIONS

In this paper, we have presented results on the progenitor metallicities of CC SNe derived through analysis of emission line spectra of

H II regions in the immediate vicinity of the explosion sites. Overall, we find only marginal evidence for a progenitor metallicity difference between SNIb and SNIa, in the sense that the mean values are slightly higher for the SNIb. There is a large overlap in metallicities between the two classes with no clear transition metallicity from SNIa to SNIb and with both SN types being found in considerable numbers at all metallicities probed by the current study.

ACKNOWLEDGMENTS

We thank the referee F. Mannucci for his constructive comments and suggestions on the paper. MH acknowledges support from Fondecyt through grant 1060808, Centro de Astrofísica FONDAP 15010003, Center of Excellence in Astrophysics and Associated Technologies (PFB 06). JA and MH acknowledge support from the Millennium Center for Supernova Science through grant P06-045-F. This research has made use of the NASA/IPAC Extragalactic Data base (NED) which is operated by the Jet Propulsion Laboratory, California Institute of Technology, under contract with the National Aeronautics and Space Administration. We also acknowledge the use of the HyperLeda data base (<http://leda.univ-lyon1.fr>).

REFERENCES

- Allende Prieto C., Lambert D. L., Asplund M., 2001, *ApJ*, 556, L63
- Anderson J. P., James P. A., 2008, *MNRAS*, 390, 1527 (AJ08)
- Anderson J. P., James P. A., 2009, *MNRAS*, 399, 559 (AJ09)
- Arcavi I. et al., 2010, preprint (arXiv e-prints)
- Asplund M., Grevesse N., Sauval A. J., Allende Prieto C., Kiselman D., 2004, *A&A*, 417, 751
- Baldwin J. A., Phillips M. M., Terlevich R., 1981, *PASP*, 93, 5
- Barbon R., Ciatti F., Rosino L., 1979, *A&A*, 72, 287
- Barbon R., Buondi V., Cappellaro E., Turatto M., 2009, *VizieR Online Data Catalog*, 1, 2024
- Bartunov O. S., Makarova I. N., Tsvetkov D. I., 1992, *A&A*, 264, 428
- Blaauw A., 1961, *Bull. Astron. Inst. Netherlands*, 15, 265
- Boissier S., Prantzos N., 2009, *A&A*, 503, 137 (BP09)
- Cardelli J. A., Clayton G. C., Mathis J. S., 1989, *ApJ*, 345, 245
- Covarrubias R. A., 2007, PhD thesis, Univ. Washington
- Crowther P. A., 2007, *ARA&A*, 45, 177
- Eldridge J. J., Tout C. A., 2004, *MNRAS*, 353, 87
- Eldridge J. J., Izzard R. G., Tout C. A., 2008, *MNRAS*, 384, 1109
- Filippenko A. V., 1982, *PASP*, 94, 715
- Filippenko A. V., 1997, *ARA&A*, 35, 309
- Garnett D. R., 2002, *ApJ*, 581, 1019
- Gaskell C. M., Cappellaro E., Dinerstein H. L., Garnett D. R., Harkness R. P., Wheeler J. C., 1986, *ApJ*, 306, L77
- Georgy C., Meynet G., Walder R., Folini D., Maeder A., 2009, *A&A*, 502, 611
- Habergham S. M., Anderson J. P., James P. A., 2010, *ApJ*, 717, 342
- Hakobyan A. A., Mamon G. A., Petrosian A. R., Kunth D., Turatto M., 2009, *A&A*, 508, 1259
- Heger A., Fryer C. L., Woosley S. E., Langer N., Hartmann D. H., 2003, *ApJ*, 591, 288
- Henry R. B. C., Worthey G., 1999, *PASP*, 111, 919
- James P. A., Anderson J. P., 2006, *A&A*, 453, 57
- James P. A. et al., 2004, *A&A*, 414, 23
- Kewley L. J., Dopita M. A., 2002, *ApJS*, 142, 35
- Kudritzki R.-P., Puls J., 2000, *ARA&A*, 38, 613
- Leloudas G., Sollerman J., Levan A. J., Fynbo J. P. U., Malesani D., Maund J. R., 2010, preprint (arXiv e-prints)
- Levesque E. M. et al., 2010a, *ApJ*, 709, L26
- Levesque E. M., Kewley L. J., Graham J. F., Fruchter A. S., 2010b, *ApJ*, 712, L26
- Meynet G., Maeder A., 2005, *A&A*, 429, 581
- Modjaz M. et al., 2008, *AJ*, 135, 1136
- Mokiem M. R. et al., 2007, *A&A*, 473, 603
- Pettini M., Pagel B. E. J., 2004, *MNRAS*, 348, L59 (PP04)
- Podsiadlowski P., Joss P. C., Hsu J. J. L., 1992, *ApJ*, 391, 246
- Prantzos N., Boissier S., 2003, *A&A*, 406, 259
- Prieto J. L., Stanek K. Z., Beacom J. F., 2008, *ApJ*, 673, 999
- Puls J. et al., 1996, *A&A*, 305, 171
- Sahu D. K., Tanaka M., Anupama G. C., Gurugubelli U. K., Nomoto K., 2009, *ApJ*, 697, 676
- Schlegel D. J., Finkbeiner D. P., Davis M., 1998, *ApJ*, 500, 525
- Smartt S. J., 2009, *ARA&A*, 47, 63
- Smartt S. J., Eldridge J. J., Crockett R. M., Maund J. R., 2009, *MNRAS*, 395, 1409
- Tanaka M. et al., 2009, *ApJ*, 700, 1680
- Thöne C. C., Michałowski M. J., Leloudas G., Cox N. L. J., Fynbo J. P. U., Sollerman J., Hjorth J., Vreeswijk P. M., 2009, *ApJ*, 698, 1307
- Tsvetkov D. Y., Pavlyuk N. N., Bartunov O. S., 2004, *Astron. Lett.*, 30, 729
- van den Bergh S., 1997, *AJ*, 113, 197
- Young D. R. et al., 2010, *A&A*, 512, 70

This paper has been typeset from a $\text{\TeX}/\text{\LaTeX}$ file prepared by the author.